International Journal of Bridge Engineering (IJBE), Vol. 3, No. 3, (2015), pp. 1-33

INTERNAL RESONANCE IN PEDESTRIAN BRIDGES

Alexander Blekherman

Medvinsky Corp. (USA)
e-mail: ablekherman@yahoo.com

ABSTRACT: The paper focuses on the excessive lateral sway motion in footbridges, induced by walking pedestrians, which can be treated as instability of a structure. For its explanation, a nonlinear problem of the dynamical behavior of an elastic pendulum is analyzed. It is shown that simultaneously applied two external vertical and lateral forces (the latter is based on a forced model whose amplitude is a function of a deck vibration) can lead to instability of a footbridge in the case of internal resonance, when the ratio between natural frequencies of vertical and lateral beam modes is about 2:1, and the natural vertical frequency is close to the vertical walking frequency. In this case an increasing control (load) parameter (a static displacement caused by pedestrians) passes through its critical value, the fast growth of the lateral mode is observed, and the vertical mode is saturated. The relation between the proposed model and a corresponding real structure is displayed on an example of a suspension footbridge. The nonlinear differential equations are deduced for describing nonlinear autoparametric coupling vibration of suspension footbridges. It is shown that the averaging nonlinear differential equations of suspension footbridges and an elastic pendulum are similar, what allows considering the latter as their model. In the case of lack coupling between modes, the same mathematical model describes parametric resonance for the lateral mode. The theoretical results of the analysis of the model and experimental measurements performed for the London Millennium Bridge, the Changi Mezzanine Bridge (Singapore) and the Solferino Bridge (Paris) are compared and discussed. Based on the above-mentioned test results, it is discussed the reason for arising a single-frequency lateral response after losing stability of the system in the case of

external vertical random excitation. It is shown that the model describes correctly the qualitative features of dynamical behavior of footbridges in the case of a wideband (or narrowband) random modal excitation.

KEYWORDS: dampers, experimental data, internal resonance, pedestrian bridges, vertical (lateral) vibrations.

1 INTRODUCTION

1.1 Lateral Vibration. In recent years, unexpected excessive bridge lateral vibrations caused by foot traffic, attracted great public attention. Some of the footbridges due to such vibrations were closed immediately after opening. It happened at the suspension Park Bridge in Kiev (1957), the Solferino Bridge (SB) in Paris [1] , the London Millennium Bridge (LMB), [2], and the T-Bridge (TB) in Tokyo [3]. The list of some footbridges with excessive lateral vibrations is shown in Table 1. Undoubtedly, this list is not complete. The scale of the problem is reflected in the most recent measurements with the excessive lateral sway, recorded on at least a dozen footbridges of different structural forms and sizes [4-9]. The focus of post-SB, LMB, TB researches has been to simulate mathematically the lateral excitation mechanism in swaying footbridges with early attempts assuming a tendency of pedestrians to synchronize pacing rate with strong vibrations [10-17], a phenomenon generally known as "synchronous lateral excitation" (SLE) or "pedestrian lock-in". In the case of the T-Bridge [3], it was suggested that some pedestrians started with random walking then synchronized their steps to the girder motions (the model of direct resonance), and this increased the lateral girder vibrations. That process is needed to be extended at a time. Thus, the model of direct resonance does not predict any sudden transition to a vibrating state but assumes a continuous increase in the vibration when the amplitude of pedestrian load is increased. The most popular variant is the semi-empirical model developed by Arup [2], based on the analysis of the LMB dynamic response. It proposed the lateral force exerted by a pedestrian to maintain balance being directly proportional to velocity of lateral vibration in fact, resulting in a force of negative damping. The net damping existing in the structure occupied by people, would vanish as pedestrians reached a critical number, causing exponentially increasing vibrations. However, some of the recent site measurements [4,5,9] have shown excessive vibrations in spite of lack of evidence of synchronization, indicating that this is not necessarily the cause. According to the site measurements on the footbridges with

excessive lateral vibrations, the following events were observed: the ratio between the frequencies of two girder modes was about 2:1, and there were conditions for the direct resonance of the vertically (or torsionally) excited mode. In Table 1, one can see that in four cases, the dominant (excited) modes were vertical and lateral, and in two cases, there were torsional and lateral. Fujino et al. [18] and Xia and Fujino [19] studied, with the experimental and analytical point of view, the model of a cable-stayed bridge characterized by vibration modes having the integer frequency ratio 2:1:1 (the vertical girder mode, lateral girder mode and symmetric in plain cable mode), and proving that internal resonance could be reached. Blekherman [20,21] used models of an elastic pendulum and double pendulum with only a vertical force to explain the phenomenon of lateral vibration caused by internal resonance in which lateral vibration was induced by vertical (or torsional) one. When the increasing control parameter exceeds its critical value (a bifurcation point), the system loses its stability followed by a rise in lateral vibration. Piccardo et al. [22] presented the detailed critical review of existing models that demonstrated the phenomenon of excessive lateral vibration. In some cases, for example, in the LMB and Clifton Suspension Bridge, the corresponding natural frequency of the lateral mode was about 0.5 Hz which is equal to half of the lateral walking frequency. Besides, the results of laboratory tests carried out at the Imperial College discovered a lateral force being a function of a lateral displacement. Using this information, Piccardo et al. [22] showed that, in the case of the lateral natural frequency of about 0.5 Hz (or about half the lateral walking frequency), the parametric resonance may occur. However, when a footbridge has the first lateral frequency more than 0.7 Hz, their model is not applicable. All of that means that for the same pedestrian load three dynamic situations can exist for a footbridge with an excessive lateral movement: either the lower lateral frequency is about 0.5 Hz (or is equal to half the lateral walking frequency), or it is approximately within the range $0.8 \sim 1.2$ Hz, or both previous situations exist simultaneously. In the present paper a model of an elastic pendulum with two simultaneously applied forces (one is an external harmonic vertical force while the other is a lateral one that is a function of a lateral displacement) are used in order to describe the excessive lateral vibrations caused by internal resonance. To solve the corresponding nonlinear differential equations, the method of multiple time scales is used. This method allows constructing the first order autonomous nonlinear differential equations and determining the steady-state solutions and their stability. Autoparametric vibrations describe the behavior of a one-mass

system with 2 DOF with quadratic nonlinearities whereas its control parameter is slowly changing. The control parameter is a static displacement caused by an external static vertical force. An elastic pendulum (in the case of a frequency ratio about 2:1) describes the phenomenon of transferring energy continuously back and forth between two modes in the case of free vibrations, and from the high frequency mode to the low frequency mode in the case of forced vibrations. It is the simplest model for describing this phenomenon for more complex systems (for example, for some footbridges). The relation between an elastic pendulum and footbridges is shown in the example of the coupled vibrations of a suspension bridge. It is shown that the elastic pendulum can be treated as a model of a footbridge, and all qualitative results obtained for the model can be used for understanding dynamics of pedestrian bridges. Using experimental data from the tests of the LMB, the Changi Mezzanine Bridge (Singapore) and the SB (Paris), it is shown that the linear models cannot describe adequately the dynamic behavior of footbridges with excessive lateral vibrations. The analysis of the model of an elastic pendulum shows the different reason for arising excessive lateral vibrations than synchronization among pedestrians.

2 MATHEMATICAL MODEL.

2.1 Equations of motion. Consider the planar motion of a mass point m attached to a still support by means of a massless linear spring of stiffness k (Fig. 1). The so-called free length, l_0, is the distance between the support and the mass point when the spring is not strained. The variables x and θ describe the extensibility of the spring and the pendulum angular motion, respectively. The present paper makes no differentiation between the angular and lateral motions. The state of stable static equilibrium corresponds to the case when x and θ equal to zero and the quantity x_{st} represents the static spring displacement due to gravity ($x_{st} = mg/k$). The vertical force P_y and lateral force P_z are applied to the mass m.
The kinetic and potential energies of the system have the following expressions;

$$T = 0.5m(\dot{x}^2 + (l+x)^2\dot{\theta}^2) \tag{1}$$

$$V = (mg + P_y)(l - (l+x)cos(\theta)) - P_z(l+x)sin(\theta) + 0.5k(x_{st}+x)^2 \tag{2}$$

where $l = l_0 + x_{st}$ and g - gravity acceleration. The Lagrangian $L = T - V$ can be written as follows:

$$\begin{aligned} L &= 0.5m(\dot{x}^2 + (l+x)^2\dot{\theta}^2) \\ &\quad -(mg + P_y)(l - (l+x)cos(\theta)) \\ &\quad +P_z(l+x)sin(\theta) - 0.5k(x_{st}+x)^2 \end{aligned} \tag{3}$$

Denoting
$u = x/l$,
$\omega_s^2 = k/m$,
$\omega_p^2 = g/l$,
and dividing the Lagrangian by the common factor ml^2, the modified Lagrangian will be

$$\begin{aligned} L1 &= 0.5(\dot{u}^2 + (1+u)^2\dot{\theta}^2) - 2(\omega_p^2 + P_y/lm)(1 - (1+u)cos(\theta)) \\ &\quad +2P_z(1+u)sin(\theta)/ml - \omega_s^2(u + \omega_p^2/\omega_s^2)^2) \end{aligned} \tag{4}$$

where ω_s - the frequency of a spring mode, ω_p - the frequency of a pendulum mode. Using Lagrange's equations and including damping terms, the following equations of motion are obtained:

$$\begin{aligned} \ddot{u} + \omega_s^2 u = &-(c_s/m)\dot{u} + (1+u)\dot{\theta}^2 - \omega_p^2(1 - cos(\theta)) \\ &+(P_y/lm)cos(\theta) + P_z sin(\theta)/lm \end{aligned} \tag{5}$$

$$(1+u)\ddot{\theta} + (\omega_p^2 + P_y/lm)sin(\theta) = -(c_p/m)\dot{\theta} - 2\dot{u}\dot{\theta} + P_z cos(\theta)/lm \tag{6}$$

where c_s, c_p - are damping coefficients for the spring mode and pendulum mode, respectively. It should be noted that the Lagrangian (4) contains the terms proportional to $u\dot{\theta}^2$ and $u\theta^2$ because $cos(\theta) = 1 - 0.5\theta^2$. The presence of those terms produce an internal resonance when ω_s is near $2\omega_p$.

According to the laboratory tests carried out at Imperial College which involved pedestrians walking on a moving platform, the lateral dynamic force applied by pedestrians is a function of a lateral displacement (Dallard et al. [23], Piccardo et al.[22]). The data were obtained during the tests performed on a harmonically moving platform with pedestrians walking with the same frequency as the platform. The dynamic load factor α, which depends on the considered harmonic load and on the load direction (Dallard et al. [23]), can be approximately expressed as follows:

$$\alpha = \alpha_0 + \alpha_1 q(t) \tag{7}$$

where α_0 is a dynamic loading factor on a stationary platform ($\alpha_0 = 0.04$), α_1 can be calculated from the data of the graph for equation (7) ($\alpha_1 \approx$

$2m^{-1}$), and q(t) is a lateral displacement of the platform. In the terms of the problem at hand α can be rewritten as

$$\alpha = \alpha_0 + \alpha_2\theta(t) \tag{8}$$

where $\alpha_2 = \alpha_1 l$.

Denoting $P_y = acos(\omega_3 t)$ and using (8), P_z can be expressed as follows:

$$P_z = (\alpha_0 + \alpha_2\theta(t))acos(\omega_4 t) \tag{9}$$

where
ω_3 is the frequency of an external vertical force,
ω_4 is the frequency of an external lateral force.

2.2 Nondimensionalization. The following nondimensionalization is adopted.

$\tau = \omega_p t$,
$\lambda_1 = \omega_s/\omega_p$,
$\lambda_2 = \omega_p/\omega_p = 1$,
$\Omega_1 = \omega_3/\omega_p$,
$\Omega_2 = \omega_4/\omega_p$,
$c_s/2m\omega_s = n_1$,
$c_p/2m\omega_p = n_2$,
$a/lm\omega_p^2 = \lambda_1^2 x_{st}/l = \lambda_1^2\rho$
where x_{st} -a static displacement from a vertical external force,
$\rho = x_{st}/l$ - nondimensional parameter.

As a the result, the following nondimensional equations can be obtained:

$$\begin{aligned} u'' + \lambda_1^2 u = -2n_1\lambda_1 u' + \lambda_2^2\theta'^2(1+u) - 0.5\lambda_2^2\theta^2 \\ +\rho\lambda_1^2 cos(\Omega_1\tau)cos(\theta) + (\alpha_0 + \alpha_2\theta)\rho\lambda_1^2 cos(\Omega_2\tau)sin(\theta) \end{aligned} \tag{10}$$

$$\begin{aligned} (1+u)\theta'' + \lambda_2^2 sin(\theta) = -2n_2\theta' - 2u'\theta' \\ -\rho\lambda_1^2 cos(\Omega_1\tau)sin(\theta) + (\alpha_0 + \alpha_2\theta)\rho\lambda_1^2 cos(\Omega_2\tau)cos(\theta) \end{aligned} \tag{11}$$

where $()'' = d^2()/d\tau^2$, $()' = d()/d\tau$, $\lambda_2 = 1$.

3 SOLUTION by PERTURBATION METHOD of MULTIPLE TIME SCALES.

Steady forced vibrations (primary resonance) are investigated in the vicinity of the stable state equilibrium of the system. Solutions for u and θ are

assumed in the following perturbation series with two different time scales [24,25].

$$u(\tau) = \varepsilon u_1(\tau_0, \tau_1) + \varepsilon^2 u_2(\tau_0, \tau_1) + \dots \tag{12}$$

$$\theta(\tau) = \varepsilon \theta_1(\tau_0, \tau_1) + \varepsilon^2 \theta_2(\tau_0, \tau_1) + \dots \tag{13}$$

where ε
is a small nondimensional parameter and $\tau_n = \varepsilon^n \tau$, n = 0, 1.

Damping coefficients and static displacement from external force are assigned so that the effects of the damping and force appear in the same perturbation equations. Thus, $n_1 = \varepsilon \xi_1$, $n_2 = \varepsilon \xi_2$, $\rho = \varepsilon^2 \nu_{st}$.

The control parameter ν_{st} is considered as a slow changing one. To make the equations more compact, the two differential operators are defined as:

$$D_0 \equiv \partial(\ )/\partial \tau_0 \tag{14}$$

$$D_1 \equiv \partial(\ )/\partial \tau_1 \tag{15}$$

By using equations (12), (13) to solve equations (10), (11) and equating coefficients of the same powers of ε, we obtain:
order ε:

$$D_0^2 u_1 + \lambda_1^2 u_1 = 0 \tag{16}$$

$$D_0^2 \theta_1 + \lambda_2^2 \theta_1 = 0 \tag{17}$$

order ε^2:

$$\begin{aligned} D_0^2 u_2 + \lambda_1^2 u_2 = &-2 D_0 D_1 u_1 - 2\xi_1 \lambda_1 D_0 u_1 + \lambda_2^2 (D_0 \theta_1)^2 \\ &-0.5 \lambda_2^2 (\theta_1)^2 + \lambda_1^2 \nu_{st} 0.5 (exp(i\Omega_1 \tau_0) + exp(-i\Omega_1 \tau_0)) \end{aligned} \tag{18}$$

$$\begin{aligned} D_0^2 \theta_2 + \lambda_2^2 \theta_2 = &-u_1 D_0^2 \theta_1 - 2 D_1 D_0 \theta_1 - 2\xi_2 D_0 \theta_1 - 2 D_0 u_1 D_0 \theta_1 \\ &+(\alpha_0 + \alpha_2 \theta_1) \nu_{st} \lambda_1^2 0.5 (exp(i\Omega_2 \tau_0) + exp(-i\Omega_2 \tau_0)) \end{aligned} \tag{19}$$

The steady-state solutions of equations (16), (17) can be obtained in the following form:

$$u_1 = A_1(\tau_1) exp(i\lambda_1 \tau_0) + \bar{A}_1(\tau_1) exp(-i\lambda_1 \tau_0) \tag{20}$$

$$\theta_1 = A_2(\tau_1) exp(i\lambda_2 \tau_0) + \bar{A}_2(\tau_1) exp(-i\lambda_2 \tau_0) \tag{21}$$

where A_1, A_2 are arbitrary functions at this level of approximation.

3.1 Internal resonance. The tuning conditions of internal resonance are described by

$$\lambda_1 = 2\lambda_2 + \varepsilon\sigma_1 \tag{22}$$

$$\Omega_1 = \lambda_1 + \varepsilon\sigma_2 \tag{23}$$

where σ_1 - internal detuning, σ_2 - external detuning.
Taking into consideration $\Omega_1 = 2\Omega_2$, using (20), (21), (22), (23) to solve equations (18), (19), and selecting secular terms the following solvability conditions will be obtained:

$$-2A_1'i\lambda_1 - 2\lambda_1^2 i\xi_1 A_1 - 1.5A_2^2 exp(-i\sigma_1\tau_1) + 0.5\lambda_1^2 v_{st} exp(i\sigma_2\tau_1) = 0 \tag{24}$$

$$\begin{aligned} -2A_2'i - 2i\xi_2 A_2 - A_1\bar{A}_2(2\lambda_1 - 1)exp(i\sigma_1\tau_1) \\ +0.5\lambda_1^2\alpha_0 v_{st} exp(i0.5(\sigma_1+\sigma_2)\tau_1) = 0 \end{aligned} \tag{25}$$

Using polar notation $A_n = 0.5a_n exp(i\beta_n)$, (n=1,2), and separating real and imaginary parts we obtain

$$-\lambda_1 a_1' - \lambda_1^2\xi_1 a_1 - 0.375a_2^2 sin(\gamma_2) + 0.5\lambda_1^2 v_{st} sin(\gamma_1) = 0 \tag{26}$$

$$\lambda_1 a_1\beta_1' - 0.375a_2^2 cos(\gamma_2) + 0.5\lambda_1^2 v_{st} cos(\gamma_1) = 0 \tag{27}$$

$$\begin{aligned} -a_2' - \xi_2 a_2 + 0.25a_1 a_2(2\lambda_1 - 1)sin(\gamma_2) \\ -0.5\lambda_1^2\alpha_0 v_{st} sin(0.5(\gamma_2 - \gamma_1)) = 0 \end{aligned} \tag{28}$$

$$\begin{aligned} a_2\beta_2' - 0.25a_1 a_2(2\lambda_1 - 1)cos(\gamma_2) \\ +0.5\lambda_1^2\alpha_0 v_{st} cos(0.5(\gamma_2 - \gamma_1)) = 0 \end{aligned} \tag{29}$$

where

$$\gamma_1 = -\beta_1 + \sigma_2\tau_1 \tag{30}$$

$$\gamma_2 = 2\beta_2 - \beta_1 - \sigma_1\tau_1 \tag{31}$$

Substituting β_1, β_2 by γ_1, γ_2 in equations (26) – (29) the following system of equations will be obtained

$$a_1' = -\lambda_1\xi_1 a_1 - 0.375a_2^2 sin(\gamma_2)/\lambda_1 + 0.5\lambda_1 v_{st} sin(\gamma_1) \tag{32}$$

$$\begin{aligned} a_2' = -\xi_2 a_2 + 0.25a_1 a_2(2\lambda_1 - 1)sin(\gamma_2) \\ -0.5\lambda_1^2\alpha_0 v_{st} sin(0.5(\gamma_2 - \gamma_1)) \end{aligned} \tag{33}$$

$$a_1\gamma_1' = \sigma_2 a_1 - 0.375a_2^2 cos(\gamma_2)/\lambda_1 + 0.5\lambda_1 v_{st} cos(\gamma_1) \tag{34}$$

$$\begin{aligned} a_2\gamma_2' = a_2(-0.375a_2^2 cos(\gamma_2)/a_1\lambda_1 + 0.5\lambda_1 v_{st} cos(\gamma_1)/a_1) \\ -a_2\sigma_1 + 0.5a_1 a_2(2\lambda_1 - 1)cos(\gamma_2) - \lambda_1^2\alpha_0 v_{st} cos(0.5(\gamma_2 - \gamma_1)) \end{aligned} \tag{35}$$

For the steady-state response, $(a_n{}' = 0, \gamma_n{}' = 0)$ the solution is given by

$$-\lambda_1\xi_1 a_1 - 0.375a_2^2 sin(\gamma_2)/\lambda_1 + 0.5\lambda_1 v_{st} sin(\gamma_1) = 0 \quad (36)$$

$$-\xi_2 a_2 + 0.25a_1 a_2(2\lambda_1 - 1)sin(\gamma_2) - 0.5\lambda_1^2\alpha_0 v_{st} sin(0.5(\gamma_2 - \gamma_1)) = 0 \quad (37)$$

$$\sigma_2 a_1 - 0.375a_2^2 cos(\gamma_2)/\lambda_1 + 0.5\lambda_1 v_{st} cos(\gamma_1) = 0 \quad (38)$$

$$a_2(\sigma_1 + \sigma_2) - 0.5a_1 a_2(2\lambda_1 - 1)cos(\gamma_2) + \lambda_1^2\alpha_0 v_{st} cos(0.5(\gamma_2 - \gamma_1)) = 0 \quad (39)$$

As it follows from the equations (10), (11), in the case of lack coupling between modes, the same mathematical model describes parametric resonance for the lateral mode, but this case was studied by Piccardo et al. [22].

4 NUMERICAL RESULTS.

For the case of internal resonance the problem is not linear and has two alternatives to solve it numerically. The first one is to solve algebraic transcendent equations (36) - (39) checking the stability of the solution for every value of a control parameter. The perturbation method of multiple time scales transforms the original nonautonomous system of equations (10) and (11) into the autonomous ones, which allow, using standard methods, to check dynamical stability of the system by constructing its Jacobian matrix, where the latter is constructed on the basis of the equations (32) - (35), and used to determine the stability of the periodic motions. If the real part of each eigenvalue of the Jacobian matrix is not positive definite, then the periodic motion is stable; otherwise it is unstable, thereby creating the condition for appearing a bifurcation point.
The second alternative is to perform numerical and bifurcation analyses of differential equations (32) − (35). The first alternative does not use initial conditions of the problem which, from a physical point of view, are important for modeling vertical and lateral fluctuations (displacements and velocities) of the system. The second alternative, however, does include them. The present paper focuses on the second alternative. To illustrate the behavior of the model, arbitrary parameters are chosen below.

In Fig. 2 the vertical a_1 (the solid line) and lateral a_2 (the dash dot line) amplitudes are plotted as functions of the control parameter v_{st} for $\sigma_1 = \sigma_2 = 0, \xi_1 = \xi_2 = 0.01$. Fig. 2 shows that the bifurcation point ($v_{st} = 0.000479$, marked by a star) causes instability of the vertical mode, and in the vicinity of the bifurcation point, the lateral amplitude increase

is observed. Four points are marked by circles are plotted for the vertical mode. The horizontal coordinates of those points are the bifurcation ones. There are two bifurcation points in the case of the increasing control parameter direction and two ones in the opposite direction. The analysis of the type of bifurcation points is beyond of the scope of the present paper. Besides, the dotted line displays the unstable behavior of the vertical mode. So after the first bifurcation point (marked by a star) the increasing control parameter does not increase the vertical respond. Furthermore, the vertical mode loses its stability, and its additional energy is transferred to the lateral mode while the vertical mode becomes constant after the second bifurcation point. It can be treated as the vertical mode pumps the lateral mode. Fig. 2 also exhibits bistability for both modes, i.e. depending on initial conditions at a given control parameter the system might develop to more than one stable state. An increase of detuning between vertical and lateral frequencies leads to a shift of a bifurcation point, which results in an increase of the critical load. Fig. 3 shows that considerable detuning $\sigma_1 = -0.18, (\sigma_2 = 0, \xi_1 = \xi_2 = 0.01)$ results in a significant shift of the bifurcation point. In order to achieve stability of a footbridge, one of the most direct solutions is to utilize supplemental viscous damping devices to elevate a structural damping level of a bridge. This concept is based on the premise that additional damping will have to shift the bifurcation point to the unreachable point for the given maximum pedestrian load. Fig.4 and Fig.5 show influence of vertical and lateral dampers for parameters $\sigma_1 = 0.01, \sigma_2 = 0, \xi_1 = 0.04, \xi_2 = 0.01$, and $\sigma_1 = 0.01, \sigma_2 = 0, \xi_1 = 0.01, \xi_2 = 0.04$,, respectively. Though the value of the bifurcation point in both cases is approximately the same, the behavior of the system is different in the region before the bifurcation point. If the purpose of applied dampers is achieved, the lateral dampers will almost exclude the lateral movement. The simultaneous application of vertical and lateral dampers is much more effective, and it is shown in Fig.6 at parameters $\sigma_1 = 0.01, \sigma_2 = 0, \xi_1 = 0.04, \xi_2 = 0.04$. Thus, different qualitative results will be obtained applying dampers to a driven oscillator (for example, in the case of direct resonance) and doing the same for an elastic pendulum. In the first case, dampers will mitigate vibrations of the oscillator while in the second case they will shift a bifurcation point and, consequently, will increase the critical load. It also can serve for checking truthfulness of a considered model.

5 THE COUPLED VIBRATIONS of the PEDESTRIAN SUSPENSION BRIDGES.

Before it was written that Lagrangian (4) contained the terms proportional to $u\theta^2$ and $u\dot{\theta}^2$. Mandelstam et al.[26] noted that these terms would exist in the Lagrangian of all autoparametric systems (with the frequency ratio equal to 2:1), not just an elastic pendulum.

In the present paper the relation between the proposed model and a real structure is illustrated by the example of a suspension bridge (Fig. 7). It assumed that the bridge has inextensible suspenders, and its deck has two axes of symmetry.

Lateral vibrations of such bridges can occur without torsion. For the analysis of those vibrations the Lagrangian equations are used in the following form:

$$\frac{d}{dt}\frac{\partial T}{\partial \dot{q}_i} - \frac{\partial T}{\partial q_i} + \frac{\partial V}{\partial q_i} = 0 \tag{40}$$

where T and V are kinetic and potential energy, respectively, and q_i - principal coordinates. Let us denote the vertical displacement of a deck by y, and the angle, as a result of the lateral displacement, by θ. The kinematic scheme of displacements is accepted according to Fig. (8). The solutions of the equations (40) can be express in the form:

$$y(x,t) = \psi_1(x)q_1(t) \tag{41}$$

$$\theta(x,t) = \psi_2(x)q_2(t) \tag{42}$$

where $\psi_1(x), \psi_2(x)$ are satisfied by the boundary conditions of the hinged type girder. Supposing the velocity of a vertical displacement as $\frac{\partial y}{\partial t}$, the velocity of a lateral displacement is expressed as:

$$\frac{\partial (h+y)\theta}{\partial t}, \tag{43}$$

for h =$\underline{\text{H}}$(x) + $H(x)$ = const , Fig(7).
The kinetic energy has the following expression:

$$T = 0.5\int_0^L m(x)(\frac{\partial y}{\partial t})^2\ dx + 0.5\int_0^L m(x)(\frac{\partial (h+y)\theta}{\partial t})^2\ dx \tag{44}$$

where m(x) - the distribution of the mass of a bridge per unit length.
The mass of a cable is neglected, and hangers are considered as having infinite stiffness.

Substituting the values of velocities of vertical and lateral displacement in (44), the kinetic energy can be expressed as

$$T = 0.5d_1\dot{q}_1^2 + 0.5d_2\dot{q}_2^2 + 0.5d_3q_1\dot{q}_2^2 + \cdots \tag{45}$$

where
$d_1 = \int_0^L m(x)\psi_1(x)^2\ dx = M_v$,
$d_2 = h^2\int_0^L m(x)\psi_2(x)^2\ dx = h^2M_l = J_m$,
$d_3 = 2h\int_0^L m(x)\psi_1(x)\psi_2(x)^2\ dx$
The expression for the potential energy is formed by elastic properties of a bridge, a gravitational part caused by the mass of a bridge, and the external forces. The potential energy formed by elastic properties can be calculated on the basis of one general formula:

$$0.5EJ\int_0^L (\frac{\partial^2\chi}{\partial x^2})^2\ dx \tag{46}$$

where
E - the corresponding modulus of elasticity,
J - the corresponding moment of inertia,
χ - the corresponding following displacement of a bridge.

1. the vertical displacement of a deck

$$\chi_1 = y - 0.5(h+y)\theta^2 \tag{47}$$

2. the lateral displacement of a deck

$$\chi_2 = (h+y)\theta \tag{48}$$

3. the vertical displacement of a cable

$$\chi_3 = y - 0.5(H(x)+y)\theta^2 \tag{49}$$

4. the lateral displacement of a cable

$$\chi_4 = (H(x)+y)\theta \tag{50}$$

Substituting (47) - (50) into (46), the necessary potential energy will be obtained. The potential energy for a gravitational part can be expressed as:

$$g\int_0^L m(x)(y - 0.5(h+y)\theta^2)\ dx \tag{51}$$

where
g - the gravity acceleration.
By using (47) and (48) correspondingly, the potential energy from the external vertical force $F_v(x,t)$ and the external lateral force $F_l(x,t)$ will be the following:

$$V_{F_v} = \int_0^L F_v(x,t)(y - 0.5(h+y)\theta^2)\ dx \tag{52}$$

where $F_v(x,t) = f_1(x)q_3(t)$,

$$V_{F_l} = \int_0^L F_l(x,t)((h+y)\theta)\ dx \tag{53}$$

where $F_l(x,t) = f_2(x)q_4(t)$, $f_1(x)$ and $f_2(x)$ are the distribution of vertical and lateral forces along the bridge, respectively.
Having calculated all members of the potential energy, the general following expression will be obtained:

$$V = 0.5d_4q_1^2 + 0.5d_5q_2^2 + d_6q_1q_2^2 + V_{F_v} + V_{F_l} + \cdots \tag{54}$$

where
$d_4 = 2EJ_v \int_0^L (\frac{\partial^2\psi_1(x)}{\partial(x)^2})^2\ dx$,
$d_5 = EJ_lh^2 \int_0^L (\frac{\partial^2\psi_2(x)}{\partial x^2})^2\ dx + EJ_l \int_0^L (\frac{\partial^2 H}{\partial x^2}\psi_2(x) + 2\frac{\partial H}{\partial x}\frac{\partial\psi_2(x)}{\partial x} + H\frac{\partial^2\psi_2(x)}{\partial x^2})\ dx$
$-hg \int_0^L m(x)\psi_2(x)^2\ dx$,
J_v - vertical moment of inertia of a cross-section,
J_l - lateral moment of inertia of a cross-section.

The members $q_1\dot{q}_2^2$ and $q_1q_2^2$ can be named as the specific ones. Their presence in the Lagrangian function (L = T - V) leads to the nonlinear differential equations with the quadratic nonlinearity, and as described on the model of an elastic pendulum in the presence of the special frequency ratio close to 2:1, and the external vertical resonant harmonic force of the enough value, to internal resonance. Generalizing this assertion, it can be said if the energy of a pedestrian bridge includes the specific members, the internal resonance is possible. Other words, if a pedestrian bridge (for any scheme) has the excessive lateral movement, its energy will include the specific members. Gol'denblat [27] studied the free vibrations of coupled suspension bridges, built the simplified model of a suspension bridge and found experimentally that the energy is transferred continuously back and forth between the two modes of vertical and lateral vibrations in the case

of the frequency ratio close to 2:1. Using equations (40), (45), (54) and including damping terms, the following equations of motion are obtained:

$$\begin{aligned} \ddot{q_1} + \overline{\omega_1}^2 q_1 = &-\tfrac{\overline{c_1}}{M_v}\dot{q_1} + 0.5\tfrac{d_3}{M_v}\dot{q_2}^2 - \tfrac{d_6}{M_v}q_2^2 - \tfrac{\overline{P_y}}{M_v}cos(\hat{\Omega}_1 t) \\ &+0.5\tfrac{1}{M_v}q_2^2 cos(\hat{\Omega}_1 t)\int_0^L f_1(x)\psi_1(x)\psi_2(x)^2\ dx \\ &-\tfrac{1}{M_v}q_2 cos(\hat{\Omega}_2 t)\int_0^L f_2(x)\psi_1(x)\psi_2(x)\ dx \end{aligned} \tag{55}$$

$$\begin{aligned} (1+\tfrac{d_3}{J_m}q_1)\ddot{q_2} + \overline{\omega_2}^2 q_2 = &-\tfrac{c_2}{J_m}\dot{q_2} \\ -\tfrac{d_3}{J_m}\dot{q_1}\dot{q_2} - 2\tfrac{d_6}{J_m}q_1 q_2 + &\tfrac{h}{J_m}q_2 cos(\hat{\Omega}_1 t)\int_0^L f_1(x)\psi_2(x)^2\ dx \\ &+\tfrac{1}{J_m}q_1 q_2 cos(\hat{\Omega}_1 t)\int_0^L f_1(x)\psi_1(x)\psi_2(x)^2\ dx \\ -\tfrac{h}{J_m}\overline{P_z}cos(\hat{\Omega}_2 t) - &\tfrac{1}{J_m}q_1 cos(\hat{\Omega}_2 t)\int_0^L f_2(x)\psi_1(x)\psi_2(x)\ dx \end{aligned} \tag{56}$$

where
$\overline{\omega_1}^2 = d_4/d_1$,
$\overline{\omega_2}^2 = d_5/d_2$,
$\overline{P_y} = \int_0^L f_1(x)\psi_1(x)\ dx$,
$\overline{P_z} = \int_0^L f_2(x)\psi_2(x)\ dx$,
$q_3 = cos(\hat{\Omega}_1 t)$,
$q_4 = cos(\hat{\Omega}_2 t)$,
$\hat{\Omega}_1$ - the frequency of an external vertical force,
$\hat{\Omega}_2$ - the frequency of an external lateral force.
In the case of pedestrian bridges according to Matsumoto et al. [28], the distribution of the pedestrian mass (of the N_p pedestrians) walking with the dominant frequency Ω_1 along the bridge, commonly assumed as uniform in crowd conditions, and $\overline{P_y}$ can be rewritten as

$$\overline{P_y} = \overline{a}\int_0^L \psi_1(x)\ dx \tag{57}$$

where
$\overline{a} = g m_{ps}\sqrt{N_p}/L$,
m_{ps} - the mass of a single pedestrian,
L - the footbridge span length.
Using the equations (7), (8) and (53), the $\overline{P_z}$ in the equation (56) can be rewritten as

$$\overline{P_z} = \overline{a}(\alpha_0\int_0^L \psi_2(x)\ dx + \alpha_2 q_2(t)\int_0^L \psi_2(x)^2\ dx) \tag{58}$$

where
$\alpha_2 = h\alpha_1$

5.1 Nondimensionalization. The following nondimensionalization is adopted.

$\tau = \overline{\omega_2}t$,
$\overline{\lambda_1} = \overline{\omega_1}/\overline{\omega_2}$,
$\overline{\lambda_2} = \overline{\omega_2}/\overline{\omega_2} = 1$,
$\overline{\Omega_1} = \hat{\Omega}_1/\overline{\omega_2}$,
$\overline{\Omega_2} = \hat{\Omega}_2/\overline{\omega_2}$,
$u_1 = q_1/h$,
$u_2 = q_2$,
$\overline{c_1}/M_v\overline{\omega_1} = 2\overline{n_1}$,
$\overline{c_2}/J_m\overline{\omega_2} = 2\overline{n_2}$

As a result, the following nondimensional equations can be obtained

$$\begin{aligned}\overline{u_1}'' + \overline{\lambda_1}^2\overline{u_1} = -2\overline{n_1}\overline{\lambda_1}\overline{u_1}' + s_1\overline{u_2}'^2 - s_2\overline{u_2}^2 - k_1\overline{\rho_1}\overline{\lambda_1}^2 cos(\overline{\Omega_1}\tau) \\ +s_5\overline{u_2}^2 cos(\overline{\Omega_1}\tau) - s_6\overline{u_2}cos(\overline{\Omega_2}\tau)\end{aligned} \tag{59}$$

$$\begin{aligned}(1 + s_3\overline{u_1})\overline{u_2}'' + \overline{\lambda_2}^2\overline{u_2} = -2\overline{n_2u_2}' - s_3\overline{u_1}'\overline{u_2}' - s_4\overline{u_1u_2} \\ -\overline{\rho_1}\alpha_0\overline{\lambda_1}^2 k_2 cos(\overline{\Omega_2}\tau) - \overline{\rho_1}\alpha_2\overline{u_2}\overline{\lambda_1}^2 k_3 cos(\overline{\Omega_2}\tau) \\ +s_7\overline{u_2}cos(\overline{\Omega_1}\tau) + s_8\overline{u_1u_2}cos(\overline{\Omega_1}\tau) - s_9\overline{u_1}cos(\overline{\Omega_2}\tau)\end{aligned} \tag{60}$$

where
$()'' = d^2()/d\tau^2$, $()' = d()/d\tau$, $\lambda_2 = 1$.
$s_1 = 0.5d_3/(M_v h)$,
$s_2 = d_6/(M_v h\overline{\omega_2}^2)$,
$k_1 = \int_0^L \psi_1(x)dx/h$,
$\overline{\rho_1} = \sqrt{(N_p)}\frac{gm_{ps}}{L\overline{\omega_1}^2 M_v}$,
$k_1\overline{\rho_1} = q_{1st}/h$,
q_{1st} - a static displacement from an external vertical force,

$k_2 = M_v \int_0^L \psi_2(x)dx/M_l h$,
$k_3 = M_v \int_0^L \psi_2(x)^2 dx/M_l h$,
$k_2\overline{\rho_1} = (k_2/k_1)(q_{1st}/h)$ if $k_1 \neq 0$,
$s_3 = d_3 h/J_m$,
$s_4 = 2d_6 h/(J_m\overline{\omega_2}^2)$,
$s_5 = 0.5\int_0^L f_1(x)\psi_1(x)\psi_2(x)^2 dx/(M_v h\overline{\omega_2}^2)$,
$s_6 = \int_0^L f_2(x)\psi_1(x)\psi_2(x)dx/(M_v h\overline{\omega_2}^2)$,
$s_7 = h\int_0^L f_1(x)\psi_2(x)^2 dx/(J_m\overline{\omega_2}^2)$,
$s_8 = h\int_0^L f_1(x)\psi_1(x)\psi_2(x)^2 dx/(J_m\overline{\omega_2}^2)$,

$s_9 = h\int_0^L f_2(x)\psi_1(x)\psi_2(x)dx/(J_m\overline{\omega_2}^2)$

5.2 Solution by Perturbation Method of Multiple Time scales.
Solutions for $\overline{u_1}$ and $\overline{u_1}$ are assumed in the following perturbation series with two different time scales repeating the method which was used before.

$$\overline{u_1}(\tau) = \varepsilon u_{11}(\tau_0,\tau_1) + \varepsilon^2 u_{12}(\tau_0,\tau_1) + \dots \tag{61}$$

$$\overline{u_2}(\tau) = \varepsilon u_{21}(\tau_0,\tau_1) + \varepsilon^2 u_{22}(\tau_0,\tau_1) + \dots \tag{62}$$

where $\tau_n = \varepsilon^n$, $n = 0, 1....$
Damping coefficients and static displacement from external force are assigned so that the effects of the damping and force appear in the same perturbation equations. Thus, $\overline{n_1} = \varepsilon\xi_1$, $\overline{n_2} = \varepsilon\xi_2$, $\overline{\rho_1} = \varepsilon^2\rho_1$, $f_1 = \varepsilon^2\overline{f_1}$,$f_2 = \varepsilon^2\overline{f_2}$.
To make the equations more compact, the two differential operators are defined as:

$$D_0 \equiv \partial(\ )/\partial\tau_0 \tag{63}$$

$$D_1 \equiv \partial(\ )/\partial\tau_1 \tag{64}$$

By using equations (61), (62) to solve equations (59), (60) and equating coefficients of the same powers of ε, we obtain:
order ε:

$$D_0^2 u_{11} + \overline{\lambda_1}^2 u_{11} = 0 \tag{65}$$

$$D_0^2 u_{21} + \overline{\lambda_1}^2 u_{21} = 0 \tag{66}$$

order ε^2:

$$\begin{gathered} D_0^2 u_{12} + \overline{\lambda_1}^2 u_{12} = -2D_0D_1u_{11} - 2\overline{\lambda_1}\xi_1 D_0 u_{11} + s_1(D_0u_{21})^2 \\ -s_2u_{21}^2 - 0.5\overline{\lambda_1}^2\rho_1\exp(i\overline{\Omega_1}\tau_0) - 0.5\overline{\lambda_1}^2\rho_1\exp(-i\overline{\Omega_1}\tau_0) \end{gathered} \tag{67}$$

$$\begin{gathered} D_0^2 u_{22} + \overline{\lambda_2}^2 u_{22} = -2D_0D_1u_{21} - s_3u_{11}D_0^2u_{21} - 2\xi_2 D_0u_{21} \\ -s_3D_0u_{11}D_0u_{21} - s_4u_{11}u_{21} - 0.5\alpha_0\overline{\lambda_1}^2\rho_1k_2\exp(i\overline{\Omega_2}\tau_0) \\ -0.5\alpha_0\overline{\lambda_1}^2\rho_1k_2\exp(-i\overline{\Omega_2}\tau_0) \\ -0.5\overline{\alpha_2}\overline{\lambda_1}^2\rho_1k_3u_{21}\exp(i\overline{\Omega_2}\tau_0) - 0.5\overline{\alpha_2}\overline{\lambda_1}^2\rho_1k_3u_{21}\exp(-i\overline{\Omega_2}\tau_0) \end{gathered} \tag{68}$$

The steady-state solutions of equations (89) and (90) can be obtained in the following form:

$$u_{11} = A_1(\tau_1)\exp(i\overline{\lambda}_1\tau_0) + \overline{A}_1(\tau_1)\exp(-i\overline{\lambda}_1\tau_0) \tag{69}$$

$$u_{21} = A_2(\tau_1)\exp(i\overline{\lambda}_2\tau_0) + \overline{A}_2(\tau_1)\exp(-i\overline{\lambda}_2\tau_0) \tag{70}$$

where $A_1(\tau_1)$ and $A_2(\tau_1)$ are arbitrary functions at this level of approximation.

5.3 Internal resonance. The tuning conditions of internal resonance are described by

$$\overline{\lambda}_1 = 2\overline{\lambda}_2 + \varepsilon\sigma_1 \tag{71}$$

$$\overline{\Omega}_1 = \overline{\lambda}_1 + \varepsilon\sigma_2 \tag{72}$$

where σ_1 - internal detuning, σ_2 - external detuning.
Taking into consideration $\overline{\Omega}_1 = 2\overline{\Omega}_2$, using (69) - (72) to solve equations (67), (68), and selecting secular terms, the following solvability conditions will be obtained:

$$\begin{gathered}-2A_1'i\overline{\lambda}_1 - 2\overline{\lambda}_1^2 i\xi_1 A_1 - (s_1+s_2)A_2^2 exp(-i\sigma_1\tau_1) \\ -0.5\overline{\lambda}_1^2\rho_1 exp(i\sigma_2\tau_1) = 0\end{gathered} \tag{73}$$

$$\begin{gathered}-2A_2'i - 2i\xi_2 A_2 - A_1\bar{A}_2(s_3(\overline{\lambda}_1 - 1) + s_4)exp(i\sigma_1\tau_1) \\ -0.5\alpha_0\overline{\lambda_1}^2\rho_1 k_2 exp(i0.5(\sigma_1+\sigma_2)\tau_1) = 0\end{gathered} \tag{74}$$

Using polar notation $A_n = 0.5a_n exp(i\beta_n)$, (n=1,2), and separating real and imaginary parts we obtain

$$-\overline{\lambda}_1 a_1' - \overline{\lambda}_1^2\xi_1 a_1 - 0.25(s_1+s2)a_2^2 sin(\gamma_2) - 0.5\overline{\lambda}_1^2\rho_1 sin(\gamma_1) = 0 \tag{75}$$

$$\overline{\lambda}_1 a_1\beta_1' - 0.25(s_1+s_2)a_2^2 cos(\gamma_2) - 0.5\overline{\lambda}_1^2\rho_1 cos(\gamma_1) = 0 \tag{76}$$

$$\begin{gathered}-a_2' - \xi_2 a_2 + 0.25(s_3(\overline{\lambda}_1 - 1) + s_4)a_1 a_2 sin(\gamma_2) \\ +0.5\alpha_0\overline{\lambda_1}^2\rho_1 k_2 sin(0.5(\gamma_2 - \gamma_1)) = 0\end{gathered} \tag{77}$$

$$\begin{gathered}a_2\beta_2' - 0.25(s_3(\overline{\lambda}_1 - 1) + s_4)a_1 a_2 cos(\gamma_2) \\ -0.5\alpha_0\overline{\lambda_1}^2\rho_1 k_2 cos(0.5(\gamma_2 - \gamma_1)) = 0\end{gathered} \tag{78}$$

where

$$\gamma_1 = -\beta_1 + \sigma_2\tau_1 \tag{79}$$

$$\gamma_2 = 2\beta_2 - \beta_1 - \sigma_1\tau_1 \tag{80}$$

Substituting β_1, β_2 by γ_1, γ_2 in the equations (75) – (78), the following system of equations will be obtained

$$a_1' = -\overline{\lambda}_1\xi_1 a_1 - 0.25(s_1+s_2)a_2^2 sin(\gamma_2)/\overline{\lambda}_1 - 0.5\overline{\lambda}_1\rho_1 sin(\gamma_1) \tag{81}$$

$$a_2' = -\xi_2 a_2 + 0.25(s_3(\overline{\lambda}_1 - 1) + s_4)a_1 a_2 sin(\gamma_2) \\ +0.5\alpha_0 \overline{\lambda_1}^2 \rho_1 k_2 sin(0.5(\gamma_2 - \gamma_1)) \tag{82}$$

$$a_1\gamma_1' = \sigma_2 a_1 - 0.25(s_1 + s_2)a_2^2 cos(\gamma_2)/\overline{\lambda}_1 - 0.5\overline{\lambda}_1 \rho_1 cos(\gamma_1) \tag{83}$$

$$a_2\gamma_2' = a_2(-0.25(s_1 + s_2)a_2^2 cos(\gamma_2)/a_1\overline{\lambda}_1 - 0.5\overline{\lambda}_1 \rho_1 cos(\gamma_1)/a_1) \\ -a_2\sigma_1 + 0.5(s_3(\overline{\lambda}_1 - 1) + s_4)a_1 a_2 cos(\gamma_2) \\ +\alpha_0 \overline{\lambda_1}^2 \rho_1 k_2 cos(0.5(\gamma_2 - \gamma_1)) \tag{84}$$

The four equations (81) - (84) can be treated as the averaging equations because the method of averaging and the method of multiple scales are equivalent. Comparing the averaging equations (32) - (35) (an elastic pendulum) and the averaging equations (81) - (84), one can see that their structures are the same and they are differed only by the constant coefficients for nonlinear terms. It means that the qualitative features of both systems are the same, and as a consequence, an elastic pendulum describes the qualitative features of dynamic behavior of suspension footbridges.
Moreover, studying internal resonance for a double pendulum (coupled torsional and lateral modes), Blekherman [21] showed that its averaging equations were similar to the averaging equations of an elastic pendulum (coupled vertical and lateral modes).
As a result, all systems of nonlinear differential equations, describing the dynamical behavior of corresponding physical models with 2 degree of freedom providing appearance of internal resonance for the frequency ratio 2:1, are reduced to the same system of nonlinear averaging differential equations. Complementing Mandelstam et al. [26], one can say that a mathematical model of the all above-mentioned systems with autoparametric coupling is the same. As consequence, an elastic pendulum can be treated as a model describing qualitative features of all pedestrian bridges with autoparametric coupling (two coupled modes).

6 EXPERIMENTAL DATA.

It is worth noting that dynamic loading from human walk is primarily vertical with the frequency range 1.5 - 2.3 Hz. If a vertical (or torsional) natural frequency gets into this range the resonant vertical vibration can be induced by pedestrians. This type of vibrations with noticeable amplitudes occurred in many bridges (Wheeler [29], Bachmann et al. [8]). The magnitude of the lateral force (with the dominate frequency two times less than the vertical dominant one) from a human walk is smaller by one order than the vertical force and usually it was not taken into consideration. However,

the situation was changed when lateral vibrations in bridges have occurred. The excessive lateral vibrations were observed in a number of footbridges (Table 1) and there are a few site tests described in the literature. In the present paper, for supporting the proposed model, mostly some results of the field tests of three footbridges (Dallard et al. [2, 23], Brownjohn et al. [4,5] and the Solferino Bridge) are discussed. All tests for the London Millennium Bridge (LMB), the Change Mezzanine Bridge (CMB) and the Solferino Bridge with a slowly increasing load showed the fast growth of lateral vibrations after reaching some critical number of pedestrians.

The LMB (the shallow pedestrian suspension bridge) was opened in June 2000 and closed soon after opening because of unexpected excessive swaying. The bridge consists of three spans: a central span of 144 m, a northern span of 81 m, and a southern span of 108 m. Dallard et al. (2001a) wrote, that on the day of opening, the central and southern spans moved by 70 mm and 50 mm at the frequencies 0.95 and 0.8 Hz, respectively, primarily in a horizontal plane. There was no substantial lateral movement of the northern span. Excessive vertical vibrations were not observed. As shown in Table 1, the frequency ratio for the third vertical mode of the central span and the second lateral mode of the same span is 1.89:0.95 = 2:1, providing the conditions for the appearance of internal resonance. Unfortunately, the values of vertical mode frequencies for the south and north spans were not published. Intensive testing of the bridge was carried out and showed a good agreement between calculated and measured frequencies. The authors noted a highly nonlinear overall effect from a crowd of pedestrians. A group of people walked in a circulatory route was gradually increased and the fast growth of the lateral motion was observed (Dallard et al. [2]). Accelerometers and video cameras were used to record what happened. This was the essential experiment for understanding that the bridge had parametric vibrations at the frequencies 0.475 Hz and 0.95 Hz. In another similar experiment on the north span (Dallard et al. [2]) , the fast growth of lateral vibrations was observed at the frequency 1Hz. Unfortunately, the authors did not process the records by the Fourier transform to obtain the spectrum of frequencies for lateral and vertical vibrations. In order to quantify the lateral response, Dallard et al. [23] proposed the pedestrian negative damping model for the lateral frequency range of a pedestrian load 0.7 - 1.1 Hz. However, the above-mentioned model cannot explain the excessive lateral vibration at the frequency 0.475 Hz. Besides, the lateral walking force coefficient (k) has been defined by a back analysis from the tests and cannot be applied for other footbridges. The model

cannot predict the steady-state amplitude, as it is linear. If the external force corresponding to a certain number of pedestrian is less than its critical value, there are no vibrations in a footbridge because damped free vibrations are decreased to zero, and the existing external force does not excite lateral vibrations at all, while the external force is more than its critical value, the situation is similar to an unstable linear oscillator: a small disturbance may generate indefinitely- amplifying movements. It is, perhaps, appropriate to note that on the day of opening the LMB was congested by people, and with a view of point of a linear model, the lateral vibrations are impossible at a frequency of 0.95 Hz because its corresponding mode is skew symmetric.

The Changi Mezzanine Bridge (CMB) was opened in 2002. It is a 140-m-span shallow arch footbridge that connects two passenger terminals at Changi Airport, Singapore. The preliminary studies described by Brownjohn et al. [4] showed that the first lateral vibration mode (LS1) at approximately 0.9 Hz and the first symmetric torsional mode (TS1) at approximately 1.64 Hz could be easily excited by a pedestrian movement. The mode shapes and frequencies were computed with predictions by the finite-element method (FEM).. The modes LS1 and TS1 had complex spatial forms and were calculated and compared with those obtained experimentally, and showed a good agreement. The LS1 frequency was 0.891 Hz by FEM, and 0.924 Hz from the field experiment. The TS1 frequency was 1.64 Hz by FEM, and 1.856 Hz by site testing. The spatial mode LS1 has an element of vertical component while TS1 has a significant lateral one. Brownjohn et al.[5] described the field tests on CMB with excessive lateral vibration. The analysis predicted that the critical number of pedestrian was equal to 145 people. About 150 people stepped onto the bridge in groups of 10, spaces approximately 15 sec. apart. The people were given instructions and asked to walk casually, not to walk in step, but to move at their own comfortable pace. After all the people had circulated the bridge for 3 min, there were told to stop walking and remain motionless. After free vibration was observed, walking resumed; then the people stopped for a few minutes, and then left the bridge. The envelopes of mid-span lateral and vertical acceleration response in the main chord at mid-span during the test were plotted. Before the first stop, a maximum acceleration amplitude in LS1 of 0.15 m/sec^2 was recorded, and the corresponding displacement amplitude equaled 5.5 mm. The described field test includes three consecutive important components: increasing controlled loading, construction of envelopes of lateral and vertical movements, and processing records by the

Fourier transform. In the beginning of walking, both vertical and lateral vibration levels seem to increase with pedestrian numbers, and the level of the vertical signal was much more than the level of the lateral signal. As seen from the envelopes, after reaching the number of pedestrians about 100, the level of the lateral signal continued increasing steadily, but the level of the vertical signal did not grow. Besides, the lateral amplitude response grew disproportionately to the increase in pedestrian numbers. Both these phenomena can be treated as the evidence of nonlinearity of the system, and correlation between LS1 and TS1.

Besides, the processing of records by the Fourier transform revealed existence of the single spectral lines, showing the lateral and vertical movements corresponding to the frequency 0.9 Hz but there were no such phenomena for the high-frequency mode. (It can be treated as the contradiction to the hypothesis of synchronization among pedestrians). Brownjohn et al.[5] interpreted but did not explain them as damping reduction for LS1. Thus, they discovered that a multi frequency random process was converted into single-frequency process for the lateral mode.

It is worth noting that the same phenomenon was observed during the field tests of the cable-stayed T-Bridge, Tokyo, Fujino et al.[3]. In some cases, the records of excessive lateral and vertical girder vibrations (for an uncontrolled crowd) showed their occurrence with the same frequency about 1Hz. It can be explained by internal resonance because of a spatial form of a low frequency (about 1 Hz) mode was almost two times less than the high mode vertical frequency. As a result, the excessive vertical vibrations were observed with the frequency about 1 Hz from the vertical pedestrian load with the dominant vertical frequency almost two times more. The authors discovered weak (20%) synchronization of pedestrians. A certain amount of debate continues on the question of whether or not synchronization can arise during an excessive lateral movement. The authors did not observe synchronization among people on the LMB and CMB. Brownjohn et al.[5] denied its occurrence because of absence of a sharp non-resonant peak with doubled LS1 frequency in the vertical response. It can be noted that, until now synchronization has never been observed during the field tests with a controlling crowd. Although synchronization was not observed on the LMB and CBM, it may occur for large-amplitude vibrations on some congested footbridges. However, in this case synchronization should be considered not as the reason but as the consequence of the dynamic process in the state of instability. Yet, the aim of design is to avoid instability of a bridge.

The Solferino arch footbridge located in the centre of Paris was closed

shortly after inauguration: it showed hampering lateral vibrations when carrying a crowd of people; this resulted in the need for thorough investigations of its behavior under pedestrian loading. These studies involved site testing and confirmed the existence of a phenomenon causing the high amplitude lateral vibrations. Dziuba et al.[1] published a very detailed paper about the site tests of the Solferino footbridge. Only two of a number of field experiments are mentioned in this paper. Two modes of vibration were under consideration: a high frequency (torsional) mode with the natural frequency 1.56 Hz and a low frequency (lateral) mode with the natural frequency 0.8 Hz.The separate groups of 16 and 61 pedestrians participated in the tests. They marched over the bridge with a determined pace (the frequency of excitation was 1.56 Hz, i.e. the resonant load), so there was no process of forming synchronization. As a result, the only dominant frequency (1,555 Hz) with the vertical displacement 5 mm was observed for the group of 16 pedestrians. Then the second group of 61 pedestrians marched over the bridge. The only lateral frequency 0.8 Hz was dominant (with the lateral displacement 24 mm). It means that, when the value of the vertical pedestrian load is more than its critical value. It also means the coupling between two modes of vibration where the lateral low frequency mode acts as an autoparametric vibration absorber concerning the high-frequency mode.

Other researchers (Charles and Hoorpah [30]) investigated the Solferino bridge and carried out a number of site tests for a group with the increasing number of random walking pedestrians. Results of a limited number of controlled pedestrian crowd tests indicated that there is a transition point at which a rapid increase in the lateral response is triggered, and the random lateral response is converted into a single frequency response. The transition is explained as random pedestrian walking that becomes "synchronized" when lateral bridge accelerations increase beyond 0.1 m/s^2. When pedestrians (160 people) were walking fast, the one frequency lateral resonant process was not observed. This can be treated as the evidence that the pedestrian walking frequencies is too far from the natural torsional frequency 1.56 Hz.

Thus, the site tests on the LMB, CBS and Solferino Bridge revealed some qualitative features of dynamical behavior of footbridges, which support the model of internal resonance. The footbridges had two resonant high-frequency and low-frequency modes, where the high-frequency was within the load frequency range, and the natural frequency ratio is about 2:1. In the case, when the increasing resonant load exceeded its critical value,

the lateral resonance was observed. When the increasing random pedestrian load exceeded its critical value, the fast (almost instant) transition from the lateral random process to a single- frequency process (the lateral resonance) was observed. It can be treated as the evidence of a nonlinear process, autoparametic coupling between modes and pumping the low-frequency mode by the high-frequency one. Xia and Fujino [19] performed a numerical experiment for a cable-stayed-beam structure (the model of the T-Bridge, Tokyo). Results showed that, when the vertical random excitation (a stationary random process) exceeded a critical value (there was no saturation phenomenon), the amplitude was less than in the linear case; the horizontal motions of the cable and beam were excited due to autoparametric nonlinear coupling (but there was no jump phenomenon), and autoparametric responce fluctuated almost harmonically between two limits, indicating nonstationary property, and the frequency ratio was about 2:1:1.

In this regard, it may be mentioned that most studies devoted to excessive lateral vibrations of footbridges are focused on the explanation of large amplitude vibrations. However, as demonstrated by the measured data to the CBS Bridge, the Solferino Bridge and the T-Bridge, there is a problem to explain changes of bandwidth. As mentioned above, the increase in load leads to the expansion of vertical bandwidth, which can be explained by an increase of vertical mode damping due to the increased number of pedestrians. However, the reduction in lateral bandwidth was observed during experiments on the CBS and Solferino bridges. For the possible explanation, the problem can be simplified by considering only vertical load as a wideband random process. In this case Roberts [31], for the system with autoparametric coupling, considered the small motions of the coupled system near the vicinity of the unimodal response (the lateral movements are zero), showed that the vertical mode acted essentially as a linear filter and its response was a filtered random process, i.e. in our case (because of little damping) it is a narrowband random process. It means that (because of autoparametric coupling) the vertical response acts on the lateral mode as a narrowband parametric excitation and it can be considered as time dependent modification of the stiffness of the lateral mode. Thus, regarding the lateral response, the whole coupled system acts as double filter reducing the lateral frequency band. It is well known that, if the lateral bandwidth is sufficiently small, the specific narrowband process is appeared as a lateral response with a carrier frequency close to the natural frequency (it is equal to a middle of bandwidth), and with a modulation frequency equaled

to half of difference of edges of bandwidth which is changed because of a random load. The similar model of a narrowband process was considered by Davenport [32] and Ibrahim [33]. This process is distinctly seen on the records for the lateral response on the congested T-Bridge, during experiments with the Solferino Bridge, and it explains a single frequency signal for the CBS Bridge. Another phenomenon can be seen from the measured data of the field tests. The lateral response has modulation for the congested T-Bridge, the Changi Mezzanine Bridge and the Solferino Bridge for a random crowd with increasing number of pedestrians walking in circles. However, there is no modulation (the Solferino Bridge, Charles and Hoorpah [30]) in the case of a random crowd with walking pedestrians grouped together in a straight line. As the pedestrian load is random in space and time, the phenomenon can be treated as evidence, that modulation mostly depends on the pedestrian load random in space. The additional tests are necessary to determine if in this case, the modal external excitation can act like narrowband random process. Unfortunately, the response of the corresponding high-frequency mode has been not published.

Cho et al.[34] studied the behavior of autoparametric absorber to vertical narrowband random excitation. In this case, the jump phenomenon of the cantilever mode and saturated phenomenon of the main system were shown to occur if the excitation bandwidth was sufficiently small. However, as the band was increased, the jump and saturation phenomena disappeared. Thus, a wideband random process can be interpreted as an outer load for congested footbridges. The stability analysis, performed by Cho et al. [34], showed that the equilibrium solution loses the stability by Hopf bifurcation which is the reason for arising a limit cycle. Recent studies, performed by Racic and Brownjohn [35,36], and Ingolfsson et al.[37] revealed that the vertical and lateral amplitude responses for single pedestrians are narrowband random processes with similar shapes. Ingolfsson et al.[37] claimed that their tests revealed that synchronization is not a pre-condition for the development of large amplitude lateral vibrations in footbridges.

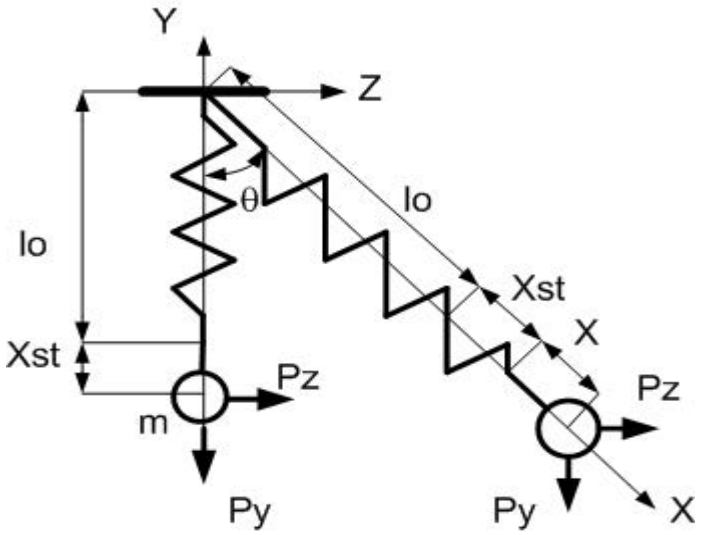

Fig.1. Physical model.

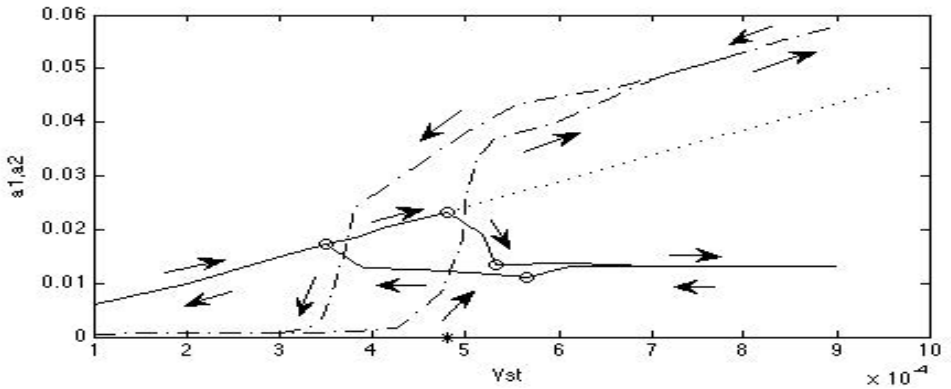

Fig.2. Vertical (a_1) and lateral (a_2) amplitudes of response as functions of control parameter ($\sigma_1 = -0.0$, $\sigma_2 = 0.0$, $\xi_1 = 0.01$, $\xi_2 = 0.01$).

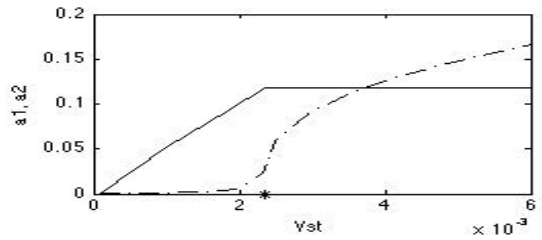

Fig.3. Vertical (a_1) and lateral (a_2) amplitudes of response as functions of control parameter ($\sigma_1 = -0.18$, $\sigma_2 = 0.0$, $\xi_1 = 0.01$, $\xi_2 = 0.01$).

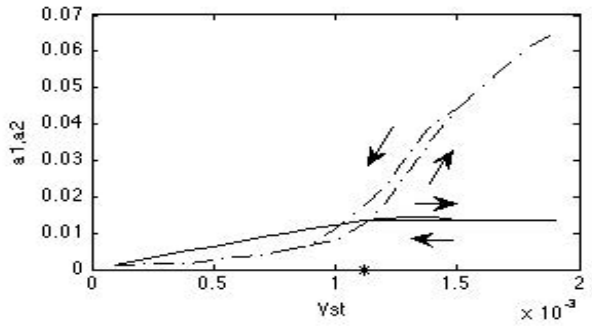

Fig.4. Vertical (a_1) and lateral (a_2) amplitudes of response as functions of control parameter ($\sigma_1 = 0.01$, $\sigma_2 = 0.0$, $\xi_1 = 0.04$, $\xi_2 = 0.01$).

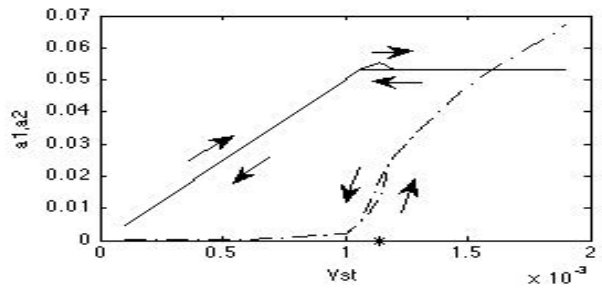

Fig.5. Vertical (a_1) and lateral (a_2) amplitudes of response as functions of control parameter ($\sigma_1 = 0.01$, $\sigma_2 = 0.0$, $\xi_1 = 0.01$, $\xi_2 = 0.04$).

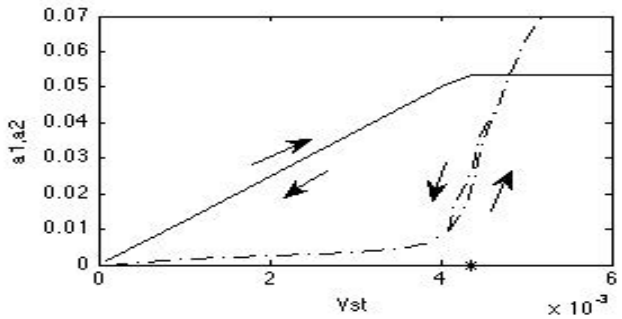

Fig.6. Vertical (a_1) and lateral (a_2) amplitudes of response as functions of control parameter ($\sigma_1 = 0.01$, $\sigma_2 = 0.0$, $\xi_1 = 0.04$, $\xi_2 = 0.04$).

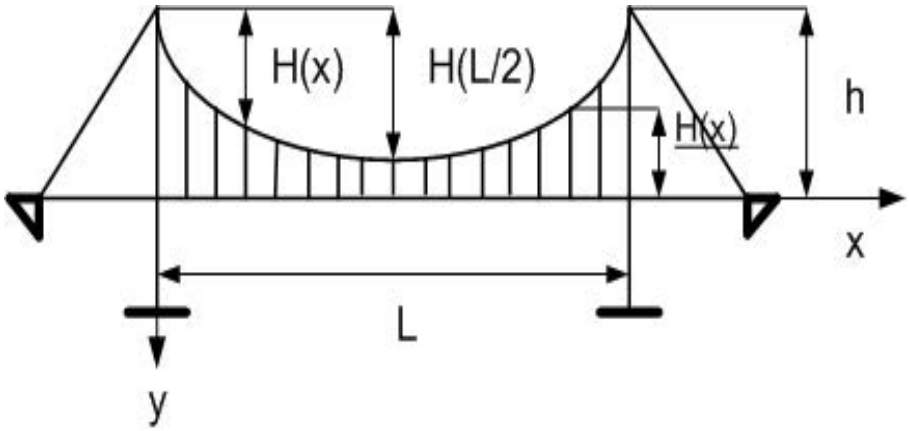

Fig.7. Suspension bridge.

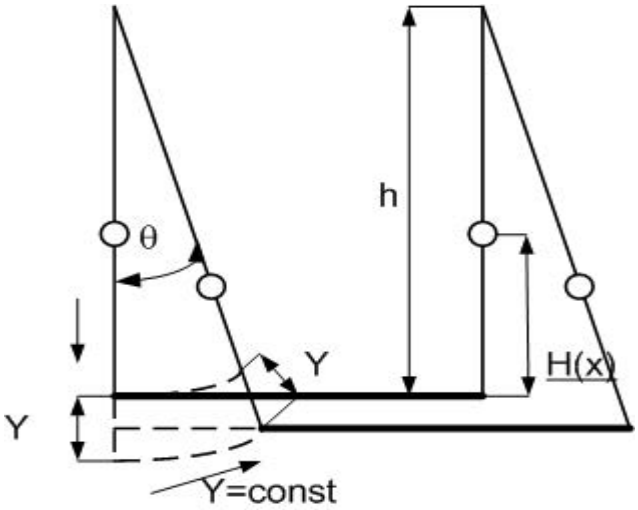

Fig.8. Kinematical scheme of possible displacements of a strained suspension bridge,o - a cable cross-section.

Table 1

Pedestrian bridges with lateral movement	Lateral mode frequency	Beam mode frequency
	Hz	Hz
The suspension bridge, 3 spans, Kiev	1	2 (vert.)
The steel arch bridge (Peterson [39])	1.1	unpublished
The concrete girder bridge (Bachman [7])	unpublished	unpublished
The T-cable-stayed bridge, Tokyo	0.9	0.7, 1.4, 2.0 (vert.)
The steel arch Solferino Bridge, Paris	0.81	1.59(torsional)
The London Millennium bridge, 3 spans	0.475,0.95-c.sp; 0.77; 1.03	1.15,1.54,1.89,2.32 (vert.)- c.span
The Link bridge, steel trusses, Birmingham (Dallard et al. [23])	0.7	unpublished
The Groves suspension bridge, UK, (Dallard et al. [23])	0.67	unpublished
The steel box girder bridge, New Zealand (Dallard et al. [23])	0.67	unpublished
The Inter-Provincial Road Bridge, steel trusses, Ottawa (Dallard et al. [23])	unpublished	unpublished
The steel arch bridge at Singapore Changi Airport, (Brownjohn et al. [5])	0.88	1.61(torsional)
The Clifton suspension bridge, UK (Mackdonald, J.H.G. [9]).	0.524, 0.746	1.642 (vert)

CONCLUSION.

Excessive lateral vibrations in pedestrian bridges under a standard excitations (a simultaneous action of a harmonic vertical force and lateral force depending on a lateral movement) were studied assuming the model of an elastic pendulum with the conditions of internal resonance. The increasing pedestrian load excited two modes of vibrations with the frequency ratio close to 2:1. The control parameter depended on a static displacement from an outer vertical force or number of pedestrians. Any increase of the control parameter past its critical value resulted in fast growth for the lateral vibrations whereas the amplitude of the vertical vibrations remained constant (saturated). The nonlinear differential equations of the forced coupling vibrations of a footbridge were deduced for a suspension bridge. It was shown that the averaging nonlinear differential equations of suspension bridges and the elastic pendulum were the same (regardless of some constant coefficients) what allowed to consider the latter (as any 2DOF system with autoparametric coupling) as their model. The same assertion is also correct for the arch bridges (Vlasov [38]). It was shown that the qualitative features of the dynamical behavior of the proposed model corresponded to the same features of the footbridges based on measurements obtained during the site tests. In the case of lack coupling between modes, the same mathematical model describes parametric resonance for the lateral mode. In the analysis a few governing parameters were under study: load, damping and detuning. The increasing detuning between vertical (torsional) and lateral frequencies leads to increase of the critical value of the pedestrian load. Dampers, in the case of internal resonance, increased the critical value of the pedestrian load while in the case of direct resonance the latter only mitigate vibrations.

The calculations showed that there was the same shift of the critical value for the vertical and lateral dampers with equal damping. It is advisable to apply lateral dampers because they are more efficient in the region before the critical value.

In the case of an external random excitation as was shown by measured data of footbridges and numerical calculations for the model, the response of a vertical (torsional) mode was a narrowband process because of small damping. For the wideband random increasing excitation, after losing stability of the system, the vertical response was increased without saturation (the T-Bridge), and it had saturation for the external narrowband random excitation, whereas the lateral response became (in both cases) a single frequency signal (with modulation), which can be treated as a specific narrowband random process. It was observed during the site tests (the Changi Mezzanine Bridge, the Solferino Bridge, and the T-Bridge), and this phenomenon corresponds to the analysis of the system with autoparametric coupling.

Despite all phenomena (qualitative features) of the dynamical behavior of the footbridges with an excessive lateral movement, described by the proposed model, are supported by experimental data, it is necessary to carry out the additional tests to determine the modal load and possible calculations. If the additional field tests show the saturation of a vertical mode, then a narrowband random process can

be adopted as a model of an external excitation for footbridges.

REFERENCES.

[1] Dziuba, P., Grilland, G., Flamand, O., Sanquirer, S., and Tetard, Y. 'La passerele Solferino. Comportement dynamique'. Bulletin Ouvrages Metalliques N 1, Office Technique pour l'Utilisation de l'Acier (OTUA), (www.otua.org), (2001), 34 - 57.
[2] Dallard, P., A.J. Fitzpatrick, A. Flint, S. Le Bourva, A. Low, R.M. Ridsdill Smith, M. Wilford. 'London millennium bridge: Pedestrian-induced lateral vibration'. J. Bridge Eng., 6(6), (2001),412 - 417.
[3] Fujino, Y., Pacheco, B. M., Nakamura, S., and Warnitchai, P. 'Synchronization of human walking observed during lateral vibration of a congested pedestrian bridge'. Earthquake Eng. Struct. Dyn., 22, (1993)741- 758.
[4] Brownjohn, James M.W., Fok, P., Roche, M., Moyo, P. 'Long span steel pedestrian bridge at Singapore Changi Airport - part 1: Prediction of vibration serviceability problems'. The Structural Engineer, 82 (16), (2004), 21- 27.
[5] Brownjohn, James M.W., Fok, P., Roche, M., Omenzetter, P. 'Long span steel pedestrian bridge at Singapore Changi Airport - part 2: Crowd loading tests and vibration mitigation measures'. The Structural Engineer, 82 (16), (2004), 28 - 34.
[6] Caetano, E., Cunha, A., Moutinho, C. 'Implementation of passive devices for vibration control at Coimbra footbridge'. In: Experimental 96 vibrational analysis for civil engineering structures EVACES, Porto, Portugal; 24-26 October, 2007.
[7] Bachman, H. 'Vibration upgrading of gymnasia, dance halls and footbridges'. Struct. Eng. Int. (IABSE, Zurich, Switzerland), 2, (1992), 118-124.
[8] Bachmann and W. Ammann. 'Vibrations in Structures Induced by Man and Machines', IABSE-AIIPC-IVBH, Structural Engineering Documents, 3e.,(1987)
[9] Macdonald, D.E. "Pedestrian-induced vibrations of the Clifton Suspension Bridge, UK", Proceedings of the Institution of Civil Engineers, Bridge Engineering 161 (2), (2008), 69 - 77.
[10] Newland, D.E. 'Pedestrian excitation of bridges'. Proceedings of the Institution of Mechanical Engineers 128, Journal of Mechanical Engineering Science, (2004), 477 - 492.
[11] Nakamura, S. "Model for lateral excitation of footbridges by synchronous walking". Journal of Structural Engineering ASCE 130 (19), (2004), 32 - 37.
[12] Roberts, T.M. "Synchronized pedestrian lateral excitation of footbridges", Proceedings Eurodyn 2005, (2005), 1089 - 1094.
[13] Roberts, T.M. "Lateral pedestrian excitation of footbridges", Journal of Bridge Engineering ASCE 10(1), (2005), 107 - 112.
[14] Roberts, T.M. "Probabilistic pedestrian lateral excitation of bridges", Proceedings of ICE, Bridge Engineering 158 (BE2), (2005), 53 - 61.
[15] Strogatz, S.H., Abrams, D.M., McRoble, A., Eckhardt, B., Ott. E. "Crowd synchrony on the Millennium Bridge". Nature (2005), 438, 43-44.
[16] Eckhardt, B., Ott. E., Strogatz, S.H., Abrams, D.M., McRoble, A. "Modeling walker synchronization on the Millennium Bridge". Physical Review E (2007),

75,021110.
[17] Venuci, F., Bruno, L. "The synchronous lateral excitation phenomenon: modeling framework and an application." C R Mec. (2007), 335, 739-745.
[18] Fujino, Y., P. Warnichai, B.M. Pacheco. "An experimental and analytical study of autoparametric resonance in a 3 DOF model of a cable-stayed beam". Nonlinear Dynamics, 4, (1993), 111 - 138.
[19] Xia, Y. and Fujino, Y. "Autoparametric resonance of a cable-stayed-beam structure under random excitation". Journal of Engineering Mechanics, ASCE, March, (2006), 279 - 286.
[20] Blekherman, A.N. "Swaying of Pedestrian Bridges". Journal of Bridge Engineering, v.10, N2, (2005), 142 - 150.
[21] Blekherman, A.N. "Autoparametric Resonance in a Pedestrian Steel Arch Bridge: Solferino Bridge, Paris". Journal of Bridge Engineering, v.12, N6, (2007), 669 - 676.
[22] Piccardo, G ., and Tubino, F. "Parametric resonance of flexible footbridges under crowd-induced lateral excitation". Journal of Sound and Vibration, 311, (2008), 353 - 371.
[23] Dallard, P., A.J.Fitzpatrick, A. Flint, S. Le Bourva, A. Low, R.M. Ridsdill Smith, M. Wilford. "The London millennium footbridge". The Structural Engineer, 79, (22), (2001) 17 - 33.
[24] Nayfeh, A.N.'Introduction to Perturbation Techniques'. (1993), Wiley, New York.
[25] Nayfeh, A.N. and Mook, D.T. ' Nonlinear Oscillations', (1995), Wiley, New York.
[26] Mandelstam, L.N., A. Vitt, G. Gorelik. 'New studies of nonlinear vibrations', (1940), Gostehizdat, Moscow.
[27] Gol'denblat, I.I. 'Contemporary problems of vibrations and stability of engineering structures', (1947), Stroiizdat, Moscow.
[28] Matsumoto, Y., T. Nishioka, H. Shiojiri, K. Matsuzaki, 'Dynamic design of footbridges', IABSE Proceedings No P-17/78, (1978), 1 - 15.
[29] Wheeler, J.E. 'Prediction and control of pedestrian-induced vibration in footbridges', J. struct. div. ASCE 108, (1982), 2045 - 2065.
[30] Charles, P., W. Hoorpah, 'Technical guide. Footbridges. Assessment of vibrational behavior of footbridges under pedestrian loading'. Setra/Afgg (French association of civil engineering) working group.(2006), Paris.
[31] Roberts, J.W., 'Random excitation of a vibratory system with autoparametric interaction', Journal of sound and vibration, 69(1)(2011), 101-116.
[32] Davenport, W.B., Jr. and Root, W.L. 'An introduction to the Theory of Random Signals and Noise', (1958). McGraw-Hill, New York.
[33] Ibrahim, R.A., 'Parametric Random Vibration', (2007). Dover Publications, Inc., Mineola, New York.
[34] Cho, D.S., C.K. Mo, G.S. Ban, K.H. Lee, 'Modal interactions in autoparametric vibration absorber to narrow band random excitation', KSME International Journal, 17(1), (2003), 97-104.
[35] Racic, V., J.M.W. Brownjohn, 'Stochastic model of near -periodic vertical

loads due to humans walking', Advanced Engineering Informatics 25, (2011), 259-275.
[36] Racic, V., J.M.W. Brownjohn, 'Mathematical modelling of random narrow band lateral excitation of footbridges due to pedestrian walking', Computers and Structures, (2012), 90-91, 116-130.
[37] Ingolfsson, E.T., C.T. Georgakis, F. Ricciardelli, J. Jonsson, 'Experimental identification of pedestrian-induced lateral forces on footbridges', Journal of Sound and Vibration, 330,(2011), 1265-1284.
[38] Vlasov, V.Z., (1963), 'Selected works', vol.2, Academy of Sciences, Moscow (Russian). [39] Peterson, C. , 'Theory of random vibrations and applications'. IT Work Rep. n 2/72, Structural Engineering Laboratory, Technical Univ. of Munich, Munich, Germany, (1972).

APPENDIX.

$$d_6 = EJ_v h \int_0^L \frac{\partial^2\psi_1(x)}{\partial x^2}\frac{\partial\psi_2(x)}{\partial x}dx + EJ_l h \int_0^L (\frac{\partial^2\psi_2(x)}{\partial x^2}\psi_2(x)\frac{\partial^2\psi_1(x)}{\partial x^2} + 2\frac{\partial^2\psi_2(x)}{\partial x^2}\frac{\partial\psi_1(x)}{\partial x}\frac{\partial\psi_2(x)}{\partial x} + \psi_1(x)(\frac{\partial^2\psi_2(x)}{\partial x^2})^2)dx - 0.5EJ_v \int_0^L (\frac{\partial^2\psi_1(x)}{\partial x^2}\psi_2(x)^2\frac{\partial^2 H}{\partial x^2} + 4\frac{\partial^2\psi_1(x)}{\partial x^2}\frac{\partial H}{\partial x}\psi_2(x) + 2\frac{\partial^2\psi_1(x)}{\partial x^2}H\frac{\partial\psi_2(x)}{\partial x})dx + EJ_l \int_0^L (\frac{\partial^2 H}{\partial x^2}\psi_2(x) + 2\frac{\partial H}{\partial x}\frac{\partial\psi_2(x)}{\partial x} + H\frac{\partial^2\psi_2(x)}{\partial x^2})(\frac{\partial^2\psi_1(x)}{\partial x^2}\psi_2(x) + 2\frac{\partial\psi_1(x)}{\partial x}\frac{\partial\psi_2(x)}{\partial x} + \psi_1(x)\frac{\partial^2\psi_2(x)}{\partial x^2})dx - 0.5g \int_0^L m(x)\psi_1(x)\psi_2(x)^2 dx$$